ISSN 1674-1056
http://cpb.iphy.ac.cn
http://iopscience.iop.org/cpb
中国物理 B
Chinese Physics
中国物理 Chinese Physics B

Theoretical prediction of the yield of strong oxides under acoustic cavitation

Jing Sun(孙晶), Zhuangzhi Shen(沈壮志), Runyang Mo(莫润阳)

Citation: Chin. Phys. B . 2019, 28(1): 014301. **doi:** 10.1088/1674-1056/28/1/014301
Journal homepage: http://cpb.iphy.ac.cn; http://iopscience.iop.org/cpb

What follows is a list of articles you may be interested in

Bidirectional asymmetric acoustic focusing with two flat acoustic metasurfaces

Di-Chao Chen(陈帝超), Xing-Feng Zhu(朱兴凤), Qi Wei(魏琦), Da-Jian Wu(吴大建)

Chin. Phys. B . 2018, 27(12): 124302. **doi:** 10.1088/1674-1056/27/12/124302

Thermoacoustic-reflected focusing lens based on acoustic Bessel-like beam with phase manipulation

An-Ru Hou(侯安茹), Wen-Ting Gao(高文婷), Jiao Qian(钱姣), Hong-Xiang Sun(孙宏祥), Yong Ge(葛勇), Shou-Qi Yuan(袁寿其), Qiao-Rui Si(司乔瑞), Xiao-Jun Liu(刘晓峻)

Chin. Phys. B . 2018, 27(12): 124301. **doi:** 10.1088/1674-1056/27/12/124301

Influence of mode conversions in the skull on transcranial focused ultrasound and temperature fields utilizing the wave field separation method: A numerical study

Xiang-Da Wang(王祥达), Wei-Jun Lin(林伟军), Chang Su(苏畅), Xiu-Ming Wang(王秀明)

Chin. Phys. B . 2018, 27(2): 024302. **doi:** 10.1088/1674-1056/27/2/024302

Broadband acoustic focusing by symmetric Airy beams with phased arrays comprised of different numbers of cavity structures

Jiao Qian(钱姣), Bo-Yang Liu(刘博阳), Hong-Xiang Sun(孙宏祥), Shou-Qi Yuan(袁寿其), Xiao-Zhu Yu(俞笑竹)

Chin. Phys. B . 2017, 26(11): 114304. **doi:** 10.1088/1674-1056/26/11/114304

Theoretical analysis of interaction between a particle and an oscillating bubble driven by ultrasound waves in liquid

Yao-Rong Wu(武耀蓉), Cheng-Hui Wang(王成会)

Chin. Phys. B . 2017, 26(11): 114303. **doi:** 10.1088/1674-1056/26/11/114303

Theoretical prediction of the yield of strong oxides under acoustic cavitation*

Jing Sun(孙晶), Zhuangzhi Shen(沈壮志)†, and Runyang Mo(莫润阳)‡

Shaanxi Normal University, Shaanxi Key Laboratory of Ultrasonics, Xi'an 710119, *China*

(Received 20 September 2018; revised manuscript received 5 November 2018; published online 30 December 2018)

Considering liquid viscosity, surface tension, and liquid compressibility, the effects of dynamical behaviors of cavitation bubbles on temperature and the amount of oxides inside the bubble are numerically investigated by acoustic field, regarding water as a work medium. The effects of acoustic frequency, acoustic pressure amplitude, and driving waveforms on bubble temperature and the number of oxides inside the bubbles by rapid collapse of cavitation bubbles are analysed. The results show that the changes of acoustic frequency, acoustic pressure amplitude, and driving waveforms not only have an effect on temperature and the number of oxides inside the bubble, but also influence the degradation species of pollution, which provides guidance for improving the degradation of water pollution.

Keywords: acoustic frequency, acoustic pressure amplitude, driving waveform, cavitation behavior, OH radical

PACS: 43.35.+d, 43.30.+m, 89.60.Ec, 82.20.–w **DOI:** 10.1088/1674-1056/28/1/014301

1. Introduction

The discharge of a large number of complex toxic and refractory organic compounds leads to water pollution which is difficult to degrade using conventional methods. Therefore, it is necessary to search for more efficient technologies to degrade such compounds. The development of innovative treatment methods encompasses the investigation of advanced oxidation processes, which are characterized by the production of strong oxides such as hydroxyl radicals. Acoustic cavitation as an advanced oxidation technology has been increasingly attempted in recent years.[1] It has some advantages compared with tradition methods, such as mild reaction conditions, a wide range of application, and not causing pollution. It is referred to as "green water treatment technology". However, this technology has not been widely applied in wastewater treatment engineering to date.

Acoustic cavitation is a kind of micro-bubble nuclei in liquids driven by ultrasonic waves. The bubble nuclei oscillate, grow, shrink, and collapse at high speed. The collapse produces a short and ultra-high temperature release, and creates high-pressure and a high-intensity electric field. Therefore, the collapse of cavitation bubbles can be likened to a "micro-reactor" at the moment of collapse, which is similar to a high-pressure "reaction kettle". The water vapor projected from the bulk liquid phase into the cavitation bubble splits and produces chain reactions at high temperature and high pressure, releasing highly active oxides (·HO, ·O, ·HOO, H_2O_2, HO_2, etc.). The organic contaminants inside the bubble will be combusted by extreme temperature and pressure and reacted by the oxides[2] and supercritical water.[3] In addition, the shock waves and microjets produced by cavitation bubbles cause oxides to escape to the interface and aqueous solution. Clearly, this leads to rapid oxidation between the oxides and organic pollutants in the solution. Due to the particularity of cavitation bubbles, the number of organic pollutants that can be degraded in the bubble is limited. Therefore, the degradation degree of organic pollutants mainly depends on the concentration of strong oxides released into the bulk solution. A great deal of previous experimental research has revealed that many factors have an effect on ultrasonic degradation, such as the solution property, the nature of contaminant, the ultrasonic field parameter, and the driving wave formation. The solution property contains viscosity,[4] surface tension,[5,6] vapor pressure,[7] ambient temperature[8] and pH,[5,9,10] etc. The characteristics of contaminant involves initial concentration of liquid,[11,12] volatility, polarity and structure of pollutant,[13] etc. The ultrasonic field parameter comprises ultrasonic frequency,[14–17] ultrasonic intensity,[12,18–20] and so on. Driving wave formation usually utilizes simple harmonic waves, square waves, and triangular waves.[21] In addition, the reactor shape also affects ultrasonic degradation. However, little has been written either at home and abroad about how these factors affect the number of strong oxides such as radicals and the number of releases to the bulk solution from the interior of bubbles.[22–26] Theoretical evidence of sewage degradation is solely based upon experiment results published in numerous research papers. In order to explore the theoretical basis of improving the degradation effect, this paper is based on the characteristics of ultrasonic field and the

*Project supported by the National Natural Science Foundation of China (Grant No. 11674207).

†Corresponding author. E-mail: szz6@163.com

‡Corresponding author. E-mail: mmrryycn@snnu.edu.cn

© 2019 Chinese Physical Society and IOP Publishing Ltd

waveform of driving ultrasonic waves. Herein we attempt to predict the aspects of the concentration (or quantity) of strong oxides, such as radicals, generated inside the bubble and to improve the methods of degradation on contaminants in water.

2. Mathematical models and numerical methods

2.1. Bubble dynamic model

The present study is aimed at modeling a cavitation bubble dynamic within an acoustic field. The section below describes the hypothesis in this modeling. i) The cavitation bubble oscillates spherically during expansion and compression, with only radial motion and without taking the influence of gravity, buoyancy, and other forces on cavitation bubbles into account. ii) We shall study in detail the specific case of an oxygen bubble in water at 20 °C and density is a constant. iii) Liquid compression, viscosity, and surface tension need to be taken into account. iv) Radiation damping should be considered. v) Heat transfer, mass transfer, diffusion of water vapor, and chemical reaction inside the bubble should be considered. vi) Heat transfer, apart from evaporation and condensation of water vapor and the effect of chemical reaction on internal energy, is not taken into consideration. The bubble motion is described by Rayleigh–Plesset's equation modified by Keller–Miksis as[27]

$$\left(1-\frac{\dot{R}}{c}\right)R\ddot{R}+\frac{3}{2}\dot{R}^2\left(1-\frac{\dot{R}}{3c}\right) = \left(1+\frac{\dot{R}}{c}\right)\frac{1}{\rho}\left(P_{\rm g}-P_t\right)+\frac{R}{\rho c}\frac{{\rm d}P_{\rm g}}{{\rm d}t}-\frac{4\mu\dot{R}}{R}-\frac{2\sigma}{\rho R}. \quad (1)$$

Here R is the radius of bubble, time derivatives are denoted by dots, $\dot{R}$ is bubble wall velocity, $\ddot{R}$ is the change rate of velocity, $\sigma = 72\times10^{-3}$ N/m is surface tension coefficient, $\mu = 10^{-6}$ m^2/s is kinematic viscosity, $c = 1500$ m/s is speed of sound in liquid, $\rho = 1000$ kg/m^3 is density of the liquid, and $P_{\rm g} = \frac{N_{\rm tot}kT}{(4\pi/3)(R^3-h^3)}$ is internal pressure in the bubble, where $N_{\rm tot}(t) = n_{\rm H_2O}(t)+n_{\rm O_2}(t)$ is the total number of water vapor and oxygen molecules inside the bubble (in the present case we study an oxygen bubble). T is temperature inside the bubble, k is Bolzmann's constant, and $h = R_0/8.54$ is Van der Waal's hard core radius. Simple harmonic wave, square wave, and triangular wave are utilized to drive cavitation:[21]

$$P_t = P_0+P_{\rm us}\sin(2\pi ft) \quad \text{(simple harmonic wave)},$$

$$P_t = P_0+\frac{4P_{\rm us}}{\pi}\sum_{j=1}^{n}\frac{(-1)^j\cos((2j+1)2\pi ft)}{2j+1} \quad \text{(square wave)},$$

$$P_t = P_0+\frac{8P_{\rm us}}{\pi^2}\sum_{j=1}^{n}\frac{(-1)^j\sin((2j+1)2\pi ft)}{(2j+1)^2} \quad \text{(triangular wave)},$$

where $P_{\rm us}$ is acoustic pressure amplitude and f is acoustic frequency.

2.2. Mass transfer across the bubble

In this paper, both oxygen and water vapor diffuse across the bubble wall during radial bubble motion.

The mass transfer of oxygen is[28]

$$n_{\rm O_2}(t+\Delta t) = n_{\rm O_2}(t)+\left.\frac{{\rm d}m}{{\rm d}t}\right|_{\rm diff}\cdot 4\pi R^2\Delta t, \quad (2)$$

$$\left.\frac{{\rm d}m}{{\rm d}t}\right|_{\rm diff} = D_{\rm O_2}\cdot\frac{c_0-c_s}{R}, \quad (3)$$

$$c_s = \frac{10^3\rho N_{\rm A}P_{\rm O_2}}{M_{\rm H_2O}K_{\rm B}} \qquad P_{\rm O_2} = \frac{n_{\rm O_2}}{N_{\rm tot}}P_{\rm g}, \quad (4)$$

where $n_{\rm O_2}(t)$ is the number of oxygen molecules, c_0 is the air concentration (in m^{-3}) in the liquid at $r=\infty$ in this calculation, $c_0 = 0$ is assumed. c_s is the saturated air concentration (in m^{-3}) in the liquid at $r = R$. $D_{\rm O_2} = 1.76\times10^9$ m^2/s is the diffusion coefficient of oxygen in liquid water, $K_{\rm B} = 6.73\times10^9$ Pa is Henry's constant of oxygen in water, $N_{\rm A}$ is Avogadro number, and $M_{\rm H_2O}$ is the molecular mass of water.

The mass transfer of water vapor is[29]

$$\begin{aligned} & n_{\rm H_2O}(t+\Delta t) \\ &= n_{\rm H_2O}(t)+4\pi R^2D_{\rm H_2O}\Delta t\left.\frac{\partial C_{\rm H_2O}}{\partial r}\right|_{r=R} \\ &= n_{\rm H_2O,0}(t)+4\pi R^2D_{\rm H_2O}\Delta t\left(\frac{C_{\rm H_2O,0}-C_{\rm H_2O,t}}{l_{\rm diff}}\right), \end{aligned} \quad (5)$$

where $n_{\rm H_2O}(t)$ is the amount of water vapor molecules inside the bubble, $D_{\rm H_2O}$ is the diffusion coefficient of water vapor, $C_{\rm H_2O,0}$ is the equilibrium concentration of water vapor at the bubble wall, $C_{\rm H_2O,t}$ is the actual concentration of water vapor inside the bubble, and $l_{\rm diff} = \min\left(\sqrt{\frac{RD_{\rm H_2O}}{|\dot{R}|}}, \frac{R}{\pi}\right)$ is the instantaneous diffusive penetration depth.

2.3. Heat transfer across the bubble

The heat transfer across the bubble is[26]

$$\frac{{\rm d}Q}{{\rm d}t} = 4\pi R^2\lambda_{\rm mix}\frac{T_0-T}{l_{\rm th}} \qquad l_{\rm th} = \min\left(\sqrt{\frac{R\chi}{\dot{R}}}, \frac{R}{\pi}\right), \quad (6)$$

where $\lambda_{\rm mix}$ is the effective thermal conductivity of mixed gases or vapor, $l_{\rm th}$ is the thermal diffusion length, χ is the thermal diffusivity of oxygen–vapor mixture in the bubble, T_0 is the temperature of bulk liquid, and T is the temperature inside the bubble.

2.4. The temperature inside the bubble

The temperature inside the bubble is[26]

$$C_{\rm V,mix}\frac{{\rm d}T}{{\rm d}t} = \frac{{\rm d}Q}{{\rm d}t}-P_{\rm g}\frac{{\rm d}V}{{\rm d}t}+\left(h_{\rm H_2O}-U_{\rm H_2O}\right)\frac{{\rm d}n_{\rm H_2O}}{{\rm d}t}. \quad (7)$$

The parameter meaning of the above equation could be attained in Refs. [30] and [31].

2.5. Chemical kinetics inside the bubble[23,24,32]

The substances inside the bubble will react chemically at high temperature and produce a series of strong oxides such as free radicals. Concentration of radicals and oxides are calculated using chemical kinetic model. In order to illustrate the model, the water molecule is split to produce ·H and ·OH at an extremely high temperature and pressure under microbubble cavitation conditions as an example:

$$H_2O \Longleftrightarrow \cdot H + \cdot OH. \tag{8}$$

$$\frac{d[\cdot OH]}{dt} = \sum \text{production} - \sum \text{destruction}, \tag{9}$$

where ·OH is the concentration of hydroxyl radical (in mol/m^3). For example, the reaction (8) in the forward direction (left to right) produces ·OH, and therefore contributes to the first sum in Eq. (9) (production $= A_f T^{b_f} \exp(-C_f/T)[H_2O]$). On the other hand, the backward process (right to left) corresponds to a consumption of ·OH and thus contributes to the second term in Eq. (9) (destruction $= A_b T^{b_b} \exp(-C_b/T)[\cdot H][\cdot OH]$). Because the cavitation bubble is an oxygen bubble, the important chemical reactions related to oxygen in the bubble are shown in Table 1. The parameters (e.g., A_f and A_b) in Eq. (9) can be found in Refs. [24] and [32].

Table 1. The important reactions inside the bubble.

Chemical reaction	Chemical reaction	Chemical reaction	Chemical reaction
$H_2O+M=OH+H+M$	$O_2+M=O+O+M$	$H_2O+O=OH+OH$	$OH+M=O+H+M$
$H+OH=O+H_2$	$H_2O+H=OH+H_2$	$HO_2+H=OH+OH$	$OH+OH+M=H_2O_2+M$
$O+OH=H+O_2$	$H+H=H_2$	$H_2O+OH=H_2O_2+H$	$H+O_2+M=HO_2+M$
$H_2O_2+H=H_2+HO_2$	$HO_2+OH=H_2O_2+O$	$O+O_2+M=O_3+M$	$OH+O_2=O_3+H$
$OH+O_2=O+HO_2$	$H+O_3=O+HO_2$	$H+O_3=OH+O_2$	$HO_2+O=OH+O_2$
$H_2O+HO_2=H_2O_2+OH$	$O_2+O_2=O_3+O$	$H_2+HO_2=H_2O_2+H$	$HO_2+H=H_2+O_2$
$O_3+HO_2=O_2+O_2+OH$			

M stands for any third body regarded as a catalyst.

2.6. Numerical simulation

The mathematical model forms a set of coupled, highly nonlinear, and stiff differential equations. In order to solve it, the Runge–Kutta method is used with Matlab.

3. Results and discussion

3.1. Cavitation bubble behavior at ultrasonic field

Ultrasonic degradation of organic pollutants requires chemical reactions, but it must occur on the basis of acoustic cavitation background. During the collapse of acoustic cavitation bubbles, the strong acoustic effects, such as transient high temperature and pressure in the bubbles, acoustic microjets and shock waves outside the bubbles, are formed. These strong acoustic effects occur mainly inside the cavitation bubble and near the bubble wall.[33] The strong sound effect of acoustic cavitation is related to the dynamic behavior of the cavitation bubble, so understanding the dynamic behavior of acoustic cavitation bubbles is helpful to explore ways and means to improve the degradation of organic pollutants by acoustic cavitation. Figure 1 shows the behavior of cavitation bubbles with a frequency of 50 kHz and an acoustic pressure amplitude of 1.2 atm. The dashed line (left scale) in Fig. 1(a) is the relationship between the radius of the cavitation bubble and time. It shows that the bubble expands first, then collapses rapidly, and then expands and collapses repeatedly. In this period, it produces high temperatures in the previous collapse stages, and soon afterwards the temperature is negligible because the collapse process is relatively weak, as shown in the solid line (right scale). In Fig. 1(b), numbers of molecules inside a bubble are shown as functions of time for one acoustic cycle. The solid line is the total number of molecules inside

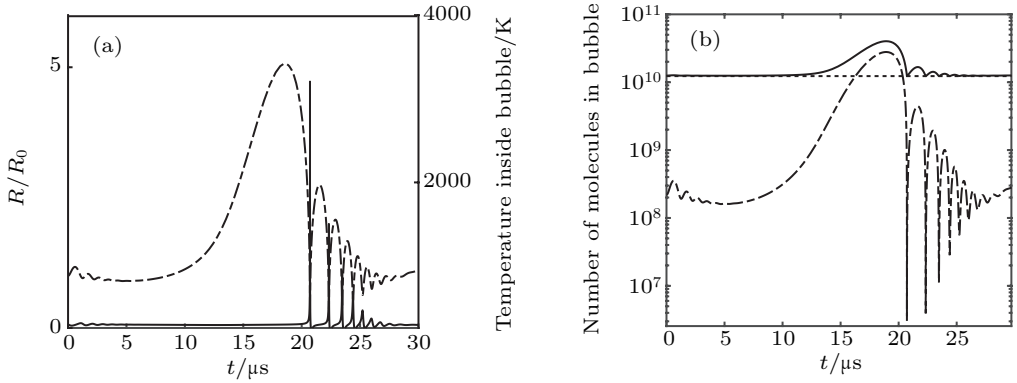


Fig. 1. Acoustic cavitation bubble behavior with a frequency of 50 kHz, an initial radius of 4 μm, and an acoustic pressure amplitude of 1.2 atm.

a bubble, the dashed-dotted line is the number of water vapor molecules (n_{H_2O}) inside a bubble, and the dashed line is the number of oxygen molecules inside a bubble. It is seen from Fig. 1(b) that the n_{H_2O} changes drastically with time due to evaporation and condensation. On the one hand, at the slow expansion phase in bubble oscillation, n_{H_2O} increases drastically by evaporation because the partial pressure of water vapor (p_v) in the bubble decreases considerably. On the other hand, at the collapse of a bubble, n_{H_2O} decreases drastically by condensation because p_v increases significantly.[22] The number of oxygen molecules do not change. Because the time scale[34] for diffusion of oxygen is $\sim R_0^2/D$ where R_0 is the initial radius of the bubble (4 μm) and D is the diffusion coefficient of oxygen in water (10^{-9} m^2/s), the time scale for oxygen diffusion is 0.01 s, which is far higher than the time scale of bubble dynamics ($1/50$ kHz $= 20$ μs). Therefore, the transport of gas across the bubble can be ignored.

3.2. The effect of acoustic frequency on yield of oxides inside the bubbles

In order to explore the effect of acoustic frequency on the behavior of cavitating bubbles and the number of strong oxides produced such as free radicals inside the bubbles, the temperature characteristics inside the bubble and the variation characteristics of the concentration of strong oxidizing substances produced by the strong acoustic effect are considered, when the acoustic pressure amplitude is 1.5 atm, and the acoustic frequencies are 25 kHz, 50 kHz, and 100 kHz, respectively. The equation (9) is a modified Arrhenius formula, which shows that the higher the temperature is, the higher the reaction rate is. Acoustic cavitation accelerates chemical reactions because of the high temperature produced by the collapse of cavitation bubbles. Therefore, it is necessary to compare the temperature variation characteristics of cavitation bubbles under different acoustic frequencies.

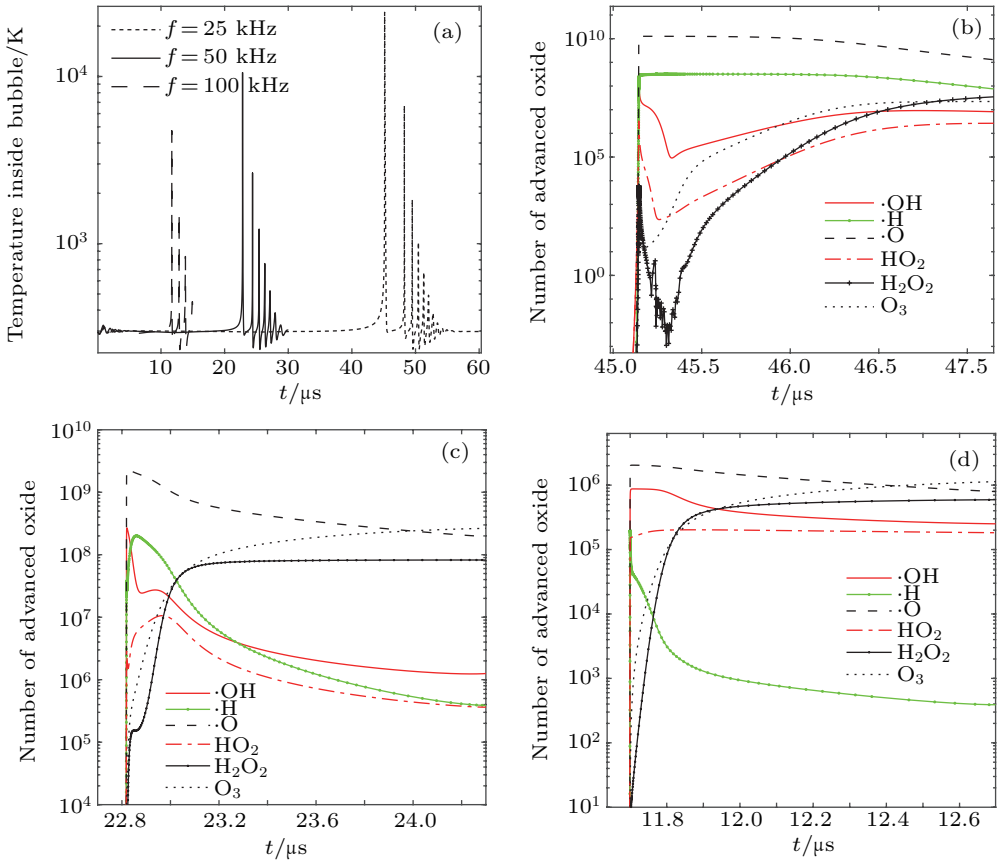


Fig. 2. The effect of frequency on the (a) temperature and (b)–(d) number of oxides inside the bubble when the acoustic pressure amplitude is 1.5 atm, the initial radius is 4 μm, and the acoustic frequencies are (b) 25 kHz, (c) 50 kHz, and (d) 100 kHz, respectively.

Figure 2(a) presents the center temperatures at 25 kHz (dotted line), 50 kHz (solid line), and 100 kHz (dash line). It is clear that the maximum center temperatures are 2.42×10^4 K (25 kHz), 1.05×10^4 K (50 kHz), and 4.73×10^3 K (100 kHz), respectively. These results show that the higher the acoustic frequency is, the lower the temperature generated by the collapse of cavitation bubbles is. Figures 2(b)–2(d) present the concentration of oxides inside bubbles at 25 kHz, 50 kHz, and 100 kHz, respectively. Here we consider the situation before the second collapse and just show the important oxides. It can be seen from the above three graphs that the higher the frequency is, the less the amount of strong oxides, such as free radicals, is produced inside bubbles. It is also shown from the above diagrams that before the second collapse, the curves

change more smoothly, and it is estimated that the amount of strong oxides inside bubbles does not change any more. Another common feature is that the strong oxides produced by the collapse of cavitation bubbles do not release into the bulk solution substantially, which results in the degradation of organic pollutants in the bulk solution depending on the nature of the organic matter. When the pollutants are volatile, they will volatilize into the bubbles during the expansion process of the cavitation bubbles. On the one hand, they will be burned off by high temperature and pressure inside the bubble. On the other hand, they will be reacted by strong oxidizing substances generated in the bubble, and also, a small part will be reacted by supercritical water generated by the gas–liquid interface. For non-volatile organic compounds (non-vocs), it mainly depends on the oxidizing substances released into the bulk solution. Therefore, compared with volatile organic compounds (vocs), the degradation effect of non-vocs is very poor, and the experiment also confirms this theoretical evidence.[7,35] By contrast, as the frequency increases, the first collapse temperature and oxide production is decreased. At 50 kHz, it can be seen that the numbers of ·OH, ·H, and HO_2 radicals decrease and the number and species of oxides dissolving into the surrounding liquid from the interior of the bubble are more than that at 20 kHz and 100 kHz. In conclusion, non-vocs in the bulk liquid are easily degraded at 50 kHz and vocs are easily degraded at 20 kHz and 100 kHz. Table 2 shows the number of oxides inside the bubble at different frequencies.

Table 2. The number of oxides inside the bubble at different frequency.

Species	$f = 25$ kHz		$f = 50$ kHz		$f = 100$ kHz	
	Initial value	Stable value	Initial value	Stable value	Initial value	Stable value
·OH	2.27×10^8	6.85×10^6	2.68×10^8	1.37×10^6	8.73×10^5	2.38×10^5
·O	1.26×10^{10}	6.92×10^8	2.32×10^9	2.41×10^8	2.04×10^6	9.92×10^6
·H	3.19×10^8	3.73×10^7	2.01×10^8	5.43×10^5	1.96×10^5	5.22×10^2
HO_2	3.34×10^6	2.46×10^6	2.84×10^6	4.43×10^5	2.03×10^5	1.91×10^5
H_2O_2	5.85×10^3	4.42×10^7	5.18×10^4	8.21×10^7	9.0×10^0	5.63×10^5
O_3	6.10×10^3	2.27×10^7	1.32×10^5	2.42×10^8	2.07×10^2	9.22×10^5

3.3. The effect of ultrasound pressure on strong oxides inside the bubbles

In Fig. 3(a), we present the changes of temperature inside the bubble for an oxygen bubble in water at a frequency of 50 kHz and pressure amplitudes of 1.2 atm (dash line), 1.5 atm (solid line), 2.0 atm (dash-and-dot line). The maximum center temperatures reach 3.2×10^3 K (1.2 atm), 1.05×10^4 K (1.5 atm), and 2.43×10^4 K (2.0 atm), respectively, and the first collapse times are 20.7 μs, 22.8 μs, and 24.9 μs, respectively. Clearly, with the increase of pressure amplitude, the collapse time delays even at the same frequency. Figures 3(b)–3(d) present the concentration of strong oxides inside the bubbles for pressure amplitudes of 1.2 atm, 1.5 atm, and 2.0 atm, respectively. Here we consider the situation before the second collapse and just show the important oxide. In Fig. 3(b), due to the small amplitude of acoustic pressure and low temperature inside the bubble, the number of strong oxidizing substances is also small. In this case, the numbers of ·OH and HO_2 do not change, the numbers of H_2O_2 and O_3 increase, whereas the number of ·O radical slightly decreases. It means that ·OH, H_2O_2, O_3, and HO_2 do not release into ambient liquid and only ·H radical absolutely releases into liquid before the second collapse. All these indicate that it is easy to degrade for vocs.

Compared with Fig. 3(b), the number of oxides in Fig. 3(c) has clearly increased, because the rise in temperature in the bubble is by nearly an order of magnitude. The figure shows that the numbers of H_2O_2 and O_3 also increase in the bubble, and the number of ·O radical decreases slightly, while the numbers of ·H, ·OH, and HO_2 decrease significantly. This trend shows that plenty of oxides have been released into the ambient liquid from the interior of the bubble, which is helpful to the degradation of non-vocs. Especially hydroxyl radical has high activity and has no selectivity to decompose organic pollutants.[36]

Due to the similar internal temperature, the order of magnitude of oxides inside the bubble is almost the same in Fig. 3(d) as in Fig. 3(c). It indicates that the degradation effect does not rise at the higher acoustic pressure. Figure 3(d) also presents that apart from ·O and ·H radicals diminishing, the rest of the oxides are released instantaneously into the bulk liquid, and then the amount increases until the second collapse. This situation will only slightly contribute to the degradation of vocs. The result obtained from the preliminary analysis of the initial and stable concentration of advanced oxides can be compared at different acoustic pressure in Table 3. Theory shows that the higher the acoustic pressure amplitude is, the better the degradation effect is, but the experimental result is not so.[37] This shows that in addition to the nature of pollutants, there will be an acoustic power value in the degradation of each pollutant to achieve the best degradation effect. After the optimal acoustic power has been reached, the effect will decrease. Perhaps, as the acoustic power increases, the number of cavitation bubbles will increase, and to a certain extent,

too many cavitation bubbles will cause the acoustic screen effect and affect the degradation effect.[38] Therefore, although the input energy is increasing, it is not certain that the effective energy acting on pollutants is increasing. So, in order to improve the degradation of organic pollutants, when the acoustic frequency is fixed and when considering the physic-chemical properties of pollutants, it is necessary to choose the best acoustic pressure amplitude, to avoid that acoustic pressure is either too low or too high, thereby affecting the treatment effect.

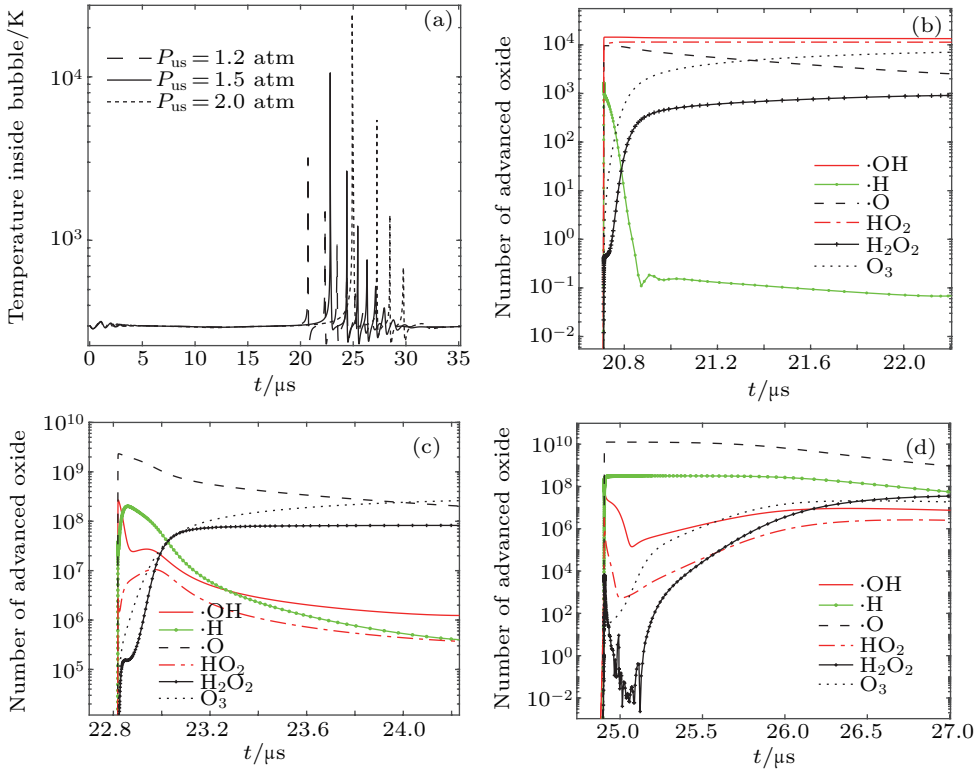


Fig. 3. The effect of acoustic pressure amplitude on the (a) temperature and (b)–(d) number of oxides inside the bubble at a frequency of 50 kHz, an initial radius of 4 μm, and pressure amplitudes of (b) 1.2 atm, (c) 1.5 atm, (d) 2.0 atm, respectively.

Table 3. The number of oxides inside the bubble at different acoustic pressure.

Species	$P_{us} = 1.2$ atm		$P_{us} = 1.5$ atm		$P_{us} = 2.0$ atm	
	Initial value	Stable value	Initial value	Stable value	Initial value	Stable value
·OH	1.44×10^4	1.34×10^4	2.68×10^8	1.37×10^6	2.20×10^8	7.56×10^8
·O	9.56×10^3	2.45×10^3	2.32×10^9	2.41×10^8	1.25×10^{10}	9.48×10^8
·H	1.64×10^3	0.00×10^0	2.01×10^8	5.43×10^5	3.17×10^8	5.67×10^7
HO_2	1.14×10^4	1.31×10^4	2.84×10^6	4.43×10^5	3.34×10^6	2.53×10^6
H_2O_2	0.00×10^0	9.08×10^2	5.18×10^4	8.21×10^7	6.27×10^3	3.58×10^7
O_3	5.00×10^0	7.09×10^3	1.32×10^5	2.42×10^8	5.69×10^3	1.85×10^7

3.4. The effect of driving waveform on the yield of strong oxides inside the bubbles

In Fig. 4(a), the changes of temperature inside the bubble on rectangular wave (dash line), triangular wave (solid line), and sinusoidal wave (dash-and-dot line) are shown for 1.5 atm at 50 kHz. The maximum internal temperatures are 2.49×10^4 K (rectangular wave), 4.05×10^3 K (triangular wave), and 1.05×10^4 K (sinusoidal wave), respectively. The crash times are at 20.03 μs, 20.99 μs, and 22.82 μs, respectively. It is clear that, even if the acoustic frequency and pressure amplitude are the same, not only the temperatures inside the bubble are different, but also the collapse times are different because of the different driving waveforms. Figures 4(b)–4(d) present the concentration curve of strong oxides created inside the bubble for rectangular wave, triangular wave, and sinusoidal wave, respectively. Clearly, the number of oxides at triangular wave is far less than that at rectangular wave and sinusoidal wave at the same condition. A possible explanation from the energy point of view is that the rectangular wave has the largest acoustic power and the triangular wave has the smallest acoustic power. It is shown that the internal bubble temperature produced by the collapse of a cavitation bubble is highest with triangular waves, followed by sinusoidal waves, and that the triangular waves produce the lowest temperature. Figure 4(a) is just such a form of expression. Furthermore, comparing Fig. 4(b), Fig. 3(d), and Fig. 2(b), it is found that the variation trend of oxides created inside the bub-

bles is astonishingly similar, and the same condition appears in Fig. 4(c), Fig. 3(b), and Fig. 2(d). Perhaps there is some internal connection between them, which needs further study. Other analyses are similar to Sections 3.2 and 3.3. The results obtained from the preliminary analysis of the initial and stable concentration of advanced oxides can be compared in Table 4. These results provide a new idea for improving the production of free radicals and other oxides.

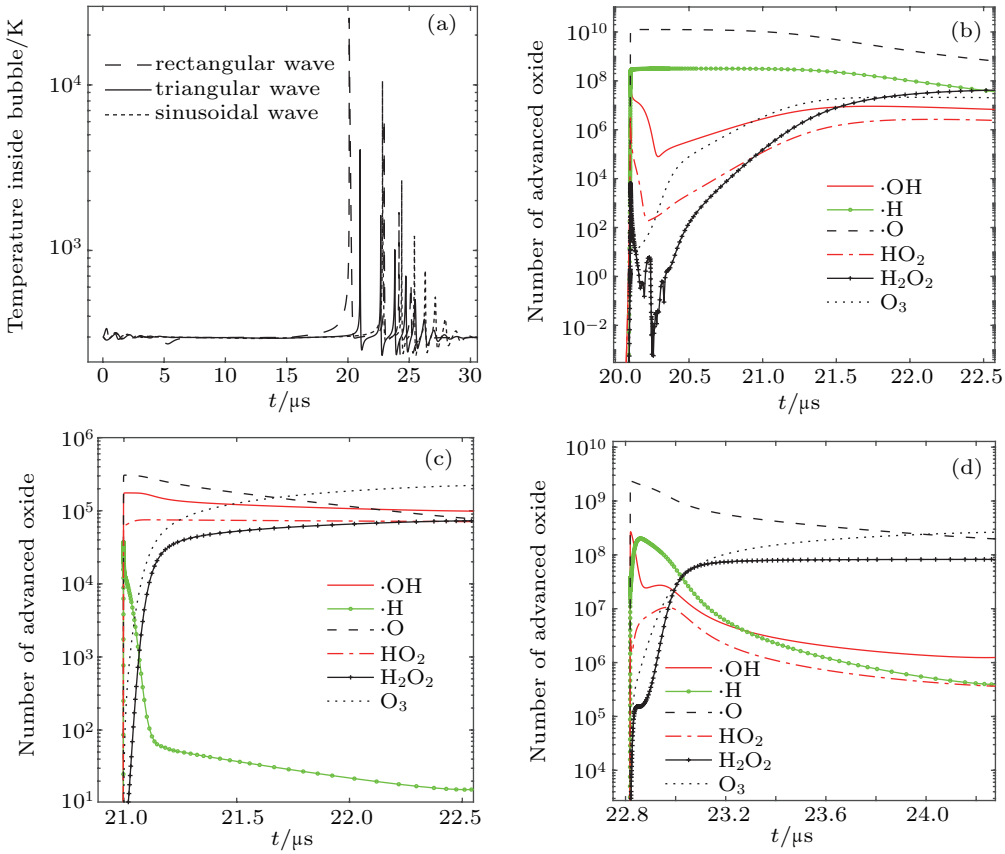


Fig. 4. The effect of driving waveform on the (a) temperature and (b)–(d) number of oxides inside the bubble at a frequency of 50 kHz, an initial radius of 4 μm, an acoustic pressure amplitude of 1.5 atm, and the driving waveforms of (b) rectangular wave, (c) triangular wave, (d) sinusoidal wave, respectively.

Table 4. The number of oxides inside the bubble at different waveform.

Species	Rectangular wave		Sinusoidal wave		Triangular wave	
	Initial value	Stable value	Initial value	Stable value	Initial value	Stable value
·OH	2.22×10^{8}	5.63×10^{6}	2.68×10^{8}	1.37×10^{6}	1.78×10^{5}	1.0×10^{5}
·O	1.26×10^{10}	4.26×10^{8}	2.32×10^{9}	2.41×10^{8}	3.12×10^{5}	8.21×10^{4}
·H	3.18×10^{8}	2.29×10^{7}	2.01×10^{8}	5.43×10^{5}	3.78×10^{4}	1.5×10^{1}
HO_2	3.34×10^{6}	1.94×10^{6}	2.84×10^{6}	4.43×10^{5}	7.57×10^{4}	7.17×10^{4}
H_2O_2	6.27×10^{3}	4.38×10^{7}	5.18×10^{4}	8.21×10^{7}	3.00×10^{0}	7.4×10^{4}
O_3	5.79×10^{3}	1.57×10^{7}	1.32×10^{5}	2.42×10^{8}	6.87×10^{2}	2.23×10^{5}

4. Conclusion

Taking liquid compressibility into consideration, we have investigated the dynamic behaviors of a single oxygen bubble and the yield of oxides produced inside the bubbles in an acoustic field by regarding water as a working medium. We can conclude that the cavitation bubble collapse is accompanied by high temperature release at the moment of compression. The amount of water vapor molecules inside the bubble increases with the slow expansion of the cavitation bubble and decreases rapidly with the instantaneous collapse. This process will occur repeatedly until the end of an acoustic cycle. But the amount of oxygen in the bubble remains constant throughout the expansion and compression stage. However, the numbers of free radicals and other oxides molecules inside the bubble depend on the temperature produced during the collapse of the cavitation bubble, and the internal temperature within the bubble is affected by the factors of acoustic frequency, acoustic pressure amplitude, driving waveform, etc. This is a complex engineering system. In order to improve the effect of ultrasonic degradation of organic pollutants,

it is necessary to consider the role of all factors comprehensively. In the article, when the acoustic pressure amplitude (1.5 atm) is constant, the acoustic frequencies are 25 kHz, 50 kHz, and 100 kHz, respectively. The number of oxides molecules inside the bubble decreases with the increase of the acoustic frequency. The acoustic waves of 25 kHz and 100 kHz are more suitable for the degradation of volatile organic pollutants, while the acoustic wave of 50 kHz is suitable for the degradation of non-volatile organic pollutants. When the acoustic frequency (50 kHz) is constant, the acoustic pressure amplitudes are 1.2 atm, 1.5 atm, and 2.0 atm, respectively. The amount of oxides inside the bubble increases with the increase of acoustic pressure amplitudes. The acoustic pressures of 1.2 atm and 2.0 atm are more suitable for the treatment of volatile organic compounds, while the acoustic pressure of 1.5 atm is more suitable for the degradation of non-volatile organic compounds. Finally, for different driving waveforms, the number of oxides created inside the bubble appears in the following order: rectangular wave $>$ sinusoidal wave $>$ triangular wave, which provides a way to research waveform driving.

References

[1] Mason T J 1926 *Chem. Ind.* **18** 47
[2] Henglein A and Kormann C 1985 *Int. J. Radiat. Biol.* **48** 251
[3] Hua L, Hochemer R H and Hoffmann M R 1995 *J. Phys. Chem.* **99** 8
[4] Gutierrez M and Henglein A 1988 *J. Phys. Chem.* **92** 2978
[5] Liu Y 1985 *Appl. Acoust.* **18** 35 (in Chinese)
[6] Suzuki Y, Maezawa A and Uchida S 1999 *Chem. Eng. Technol.* **22** 507
[7] Okuno H, Yim B, Mizukoshi Y, Nagata Y and Maeda Y 2000 *Ultrason. Sonochem.* **7** 261
[8] Ku Y, Chen K Y and Lee K C 1997 *Water Res.* **31** 929
[9] Jiang Y, Pétrier C and David W T 2002 *Ultrason. Sonochem.* **9** 163
[10] Fu M, Gao Y, Wang X H and Ding P D 2002 *Acta Scientiae Circumstantiae* **22** 402 (in Chinese)
[11] De V A, Langenhove H V and Eenoo P V 1997 *Ultrason. Sonochem.* **4** 145
[12] Ashish B and Michael C H 1994 *Environ. Sci. Technol.* **28** 1481
[13] Zhao B B and Wang L 2002 *Chem. Eng.* **21** (in Chinese)
[14] Drijvers D, De B R, De V A and Langenhove H V 1996 *Ultrason. Sonochem.* **3** S83
[15] Entezari M H, Kruus P and Otson R 1997 *Ultrason. Sonochem.* **4** 49
[16] Petrier C and Francony A 1997 *Ultrason. Sonochem.* **4** 295
[17] Cum G, Galli G, Gallo R and Spadaro A 1992 *Ultrasonics* **30** 267
[18] Price G J, Matthias P and Leoz E J 1994 *Process Saf. Environ.* **72** 27
[19] Terese M O and Philippe F B 1994 *Water Res.* **28** 1383
[20] Chen W, Fan J C, Chen L and Qian M L 2000 *China Water & Wastewater* **1** (in Chinese)
[21] Chen W Z 2014 *Acoustic Cavitation Physics* (Beijing: Science Press) p. 269
[22] Yasui K 1997 *J. Phys. Soc. Jpn.* **66** 2911
[23] Kamath V and Prosperetti A 1993 *J. Acoust. Soc. Am.* **94** 248
[24] Yasui K, Toru T, Manickam S and Yasuo I 2005 *J. Chem. Phys.* **122** 224706
[25] Li C L, Lu T and An Y 2008 *Technical Acoustics* **27** 481 (in Chinese)
[26] Toegel R, Gompf B, Pecha R and Lohse D 2000 *Phys. Rev. Lett.* **85** 3165
[27] Keller J B and Miksis M 1980 *J. Acoust. Soc. Am.* **68** 628
[28] Yasui K 1998 *Electron. Comm. Jpn. Pt. II* **81** 39
[29] Krishnan J S, Dwivedi P and Moholkar V S 2006 *Ind. Eng. Chem. Res.* **45** 1493
[30] Sivasankar T and Moholkar V S 2008 *Chemosphere* **72** 1795
[31] Sivasankar T and Moholkar V S 2009 *Chem. Eng. J.* **149** 57
[32] Yasui K, Toru T, Yasuo I and Mitome H 2003 *J. Chem. Phys.* **119** 346
[33] Suslick K S, Hammerton D A and Cline T R E 1986 *J. Am. Chem. Soc.* **108** 5641
[34] Sivasankar T, Paunikar A W and Moholkar V S 2007 *Aiche J.* **53** 1132
[35] Shemer H and Narkis N 2005 *Ultrason. Sonochem.* **12** 495
[36] Deng S F, Bai M D, Bai X Y and Liu X W 2004 *Journal of Dalian Maritime University* **30** 62 (in Chinese)
[37] F1nd1k S and Gunduz E 2006 *Ultrason. Sonochem.* **13** 203
[38] Nie G Q, Wu Y G, Li X and Wang Q H 2008 *Technology of Water Treatment* **34** 11